Analysis of Spreading of Individual Toner Particles and Levelling of Toner Layers

T. Pettersson and A. Fogden
YKI, Institute for Surface Chemistry
Stockholm, Sweden

Abstract

In the fusing of electrophotographic prints, the spreading and coalescence of individual toner particles and levelling of films are driven by surface tension and determine the optical parameters of dot gain and gloss as well as print adhesion. In this study a laboratory method has been developed to monitor in-situ the spreading of individual toner particles during heating, and extract the corresponding evolution in particle diameter and contact angle. This method was employed to study different toner particles as a function of temperature, heating rate, and substrate surface energy. Significant differences in spreading extent and rate for the different toner particles were observed, especially on higher energy surfaces, and explained in terms of their dispersive and polar interactions.

This study was combined with Xeikon printing trials using systematic variations in the fusing type and degree. The prints were analysed with interferometric profilometry to quantify the response of toner layer thickness and surface topography to the fusing conditions. In particular, spectral decomposition of surface roughness revealed interesting correlations to print gloss.

Introduction

The final step in electrophotographic printing processes involves the fusing of the transferred toner particles to the print media, e.g. paper, in the fuser system, usually by the rapid application of IR radiation and/or heated rollers. The quality of fusing, reflected in the process runnability (offset problems) and attained optical properties and adhesion of the print, is dictated by the interdependent chain of concurrent sub-processes taking place after melting of the toner particles and prior to re-solidification, including their sintering or coalescence, their spreading on the medium surface and penetration into it (if porous), and levelling of the toner film-air interface. All of these sub-processes are driven by toner surface tension effects, with the assistance of the applied thermal and mechanical energy to overcome the viscous resistance of the toner. The degree of spreading and penetration of the toner particles is dictated by their dynamic contact angle with the print medium, in turn depending on its physical characteristics, i.e. surface topography and pore space, and surface chemistry, as well as heat conduction. The development of improved printing hardware, toner systems, and media naturally relies upon a systematic understanding of this complex dynamical interplay during fusing.

Investigation of the above-mentioned sub-processes during toner fusing clearly relies upon laboratory techniques to measure both the phenomena and the component properties giving rise to them, with the aid of theoretical and empirical models to quantify the dependences. Much of our present understanding of the thermodynamics and kinetics of these sub-processes is based on the classic work of Lee[1] and other groups.[2-4] While the quantification of toner rheology, at the relatively low shear rates of relevance to fusing, is well established and reliable.[4] the determination of surface tension and energy of the toner and print medium is more challenging, as is direct measurement of particle spreading. The first part of the present study develops and applies new analytical tools to probe and predict spreading phenomena.

The optical properties of electrophotographic printed images, and in particular the gloss, vary strongly with the fusing temperature used. With a high fusing temperature the image appears glossy, whereas a lower temperature gives a matte appearance. Gloss also depends strongly on the toner layer thickness,[5] and thus can vary over an image according to the local thickness. Understanding gloss and its variations entails analysis of the effect of unfused layer thickness and fusing conditions on toner film levelling and residual surface roughness. The second part of the present study uses interferometric profilometry to quantify the unfused layer thickness and roughness of full-tone prints, their evolution during fusing, and their correlations to final gloss level.

Materials, Instruments and Methods

Spreading of Individual Toner Particles

The toner particles used in this study were C, M, Y and K from the Xeikon toner system V2. Their base polymers are 4 different polyesters, one type common to all 4 colours, another type common to M and Y, and one different type for each of C and K. Hydrophobised silica particles are present as charge control additive, lying both on the surface and within the interior of the toner particles. For the single-particle spreading measurements, these irregularly-shaped ground toner particles were transformed to spheres.[6] Particles of each colour were dispersed in glycerol, heated in a water bath to 75°C for 10 min.; the dispersion was then removed, cooled, filtered and dried under ambient conditions.

The two substrates used for the spreading experiments were clean glass (high-energy) and hydrophobically modified (low-energy) glass. The high-energy glass samples were cleaned in a plasma cleaner at medium power for 3 min. The low-energy glass was obtained by vapour phase deposition of dichlorodimethylsilane.[7]

The evolution of the covering diameter of individual spherical toner particles on clean and hydrophobised cover glass during heating was monitored in-situ. The substrate was placed on the heating cell (FDCS-196, Linkam), with corresponding control units and temperature probe. Heating was performed from ambient temperature at rate of 20°C/min. to 70°C, then held for 3 min., followed by continued heating at 10°C/min. to 125°C, held for 10 min. The spreading of the particle on the glass was viewed from above in a reflected light microscope (Nikon Optiphot-100S), with 50x lens, and CCD-camera to capture images.

Surface free energy of the 4 toners was determined by using the Fibro-DAT 1100 instrument (Fibro Systems AB) to apply 5 drops of volume 4 μl of each of the 3 test liquids, water, ethylene glycol and methylene iodide, on smooth films of the melted particles. The average value of the drop contact angle at time 1s. after contact was used to calculate the surface free energy components of the toners.

The shape of the individual toner particles after spreading was imaged and analysed with a white-light interferometric profilometer (Zygo New View 5010) operating with a 20x lens, and zoom value of 2, giving an image rectangle of 175 × 130 μm with 0.88 μm lateral resolution and a maximum resolvable surface slope of 29.5°.

Levelling of Toner Layers

Two different digital printing papers from Metsä Serla (now M-real) were used in printing trials, namely a glossy coated paper (Galilei Art Gloss, 150 g/m^2) and an uncoated paper (Galilei Opal, 160 g/m^2). The topside of the printing form contained solid print (full-tone) band fields (in the cross-direction) of 100% C, M, Y, and K, 200% blue (CM) and red (MY), 300% black (CMY), and 400% black (CMYK). Printing was performed using a Xeikon DCP 320D press with the Xeikon toner system V2. This press has two types of fusing units, one radiant source (infrared, IR) followed by two pairs of heated rolls. The press was controlled so that the four process colours achieved their Xeikon standard print density values for normal printing and fusing conditions, namely 125 and 145°C in the radiant unit and 100 and 110°C in the heated rolls, for the coated and uncoated papers, respectively. Fusing was then varied, without compensation in transferred toner amount, by using only the radiant source, only the heated nips, or the former followed by the latter. For radiant fusing only, temperature was varied in 5°C steps over the ranges 105-145°C and 120-150°C for the coated and uncoated paper, respectively. For radiant fusing followed by the heated nips, the corresponding temperature intervals investigated were 120-130°C (IR) and 95-105°C (heated rolls), for coated paper, and 140-150°C (IR) and 105-115°C (heated rolls), for uncoated paper, i.e. 5°C increase or decrease from the standard settings. Unfused samples were produced by stopping the press and cutting out samples from the unfused section of the paper web.

Surface topography of the printed papers was characterised using the same profilometer and settings as mentioned above. Stitching a 2 × 2 matrix of such adjoining rectangles provided a larger rectangle of 311 × 233 μm, maintaining the same lateral resolution. A least-squares fitted plane was subtracted to remove sample tilt. The images over these larger rectangles were FFT-filtered, either using a high(wavelength)-pass filter with lower cut-off of 5 μm or band-pass filter keeping the wavelength bands 2-5, 5-10, 10-20, 20-40, 40-200 μm. From the high-pass and band-pass filtered images the root-mean-square surface roughness *Sq* was calculated. Roughness values reported here are the mean of 4 image areas, each 311 × 233 μm. To evaluate the toner film thickness, the transition region from toner film to unprinted paper was imaged within the smaller rectangle area. The plane of least-squares fit to the unprinted region was subtracted from the entire image to give the toner film thickness from the resulting difference image. Thickness values reported here are the average of height steps from five 1-D cross-sections from one image area (175 × 130 μm).

In addition to the topographical characterization, gloss was measured on the printed and unprinted samples with a Zehntner ZGM 1020, Zehntner GmbH (Switzerland) at 75° angle using the Tappi standard as guideline.

Results and Discussion

Spreading of Individual Toner Particles

Understanding of the wetting dynamics of melted toner particles requires knowledge of both their surface tension (against air), providing one of the thermodynamic driving forces dictating spreading tendency, and their viscous forces that resist the associated flow. The rheograms of increasing and decreasing shear rate of the melted toner material for the 4 colours could each be well fitted to the Bingham approximation. The plastic viscosity and yield stress values obtained from fitting over the shear rate range 0.01–0.3 s^{-1} both display a hierarchy from K (highest) to Y to M (both quite similar) to cyan (lowest) for all temperatures over 100°C. Regarding toner surface tension, Table 1 lists the calculated values of the 3 components of their surface free energies. For all 4 toners, the dispersive (van der Waals) component is clearly dominant, as expected for these polymer materials, with the significantly smaller acid-base component most influenced by its base part. The total surface energy, as well as its non-polar (dispersive) and polar (acid-base) components, all decrease from K to C to M to Y. By way of comparison, the surface free energy of black toner measured with inverse gas chromatography gave 41 mJ/m^2 for the dispersive part.[8]

The spreading results for single particles of the 4 toners on the hydrophobised and clean glass are provided in Fig. 1. The final values of the area ratios (final/initial area), listed in

Table 2, are the mean of approx. 5 measurements for each toner–substrate pair. On the hydrophobic substrate, the temperature and time evolution of area ratio is quantitatively identical for the 4 different colours, all of which display the same onset of softening and spreading at 70°C, followed by the linear regime terminating at a plateau value of approx. 1.7 with no further increase for temperatures above 100°C.

Table 1. Surface Free Energy Components for the Different Toners and the Substrate.

Surface energy (mJ/m^2)	Total	Dispersive	Acid/Base	Base	Acid
C	34.8	33.3	1.5	5.9	0.092
M	33.4	32.2	1.2	4.0	0.093
Y	31.7	31.2	0.51	2.9	0.023
K	37.6	35.8	1.7	8.8	0.087
Hydrophobised glass	23.7	22.9	0.82	2.9	0.057

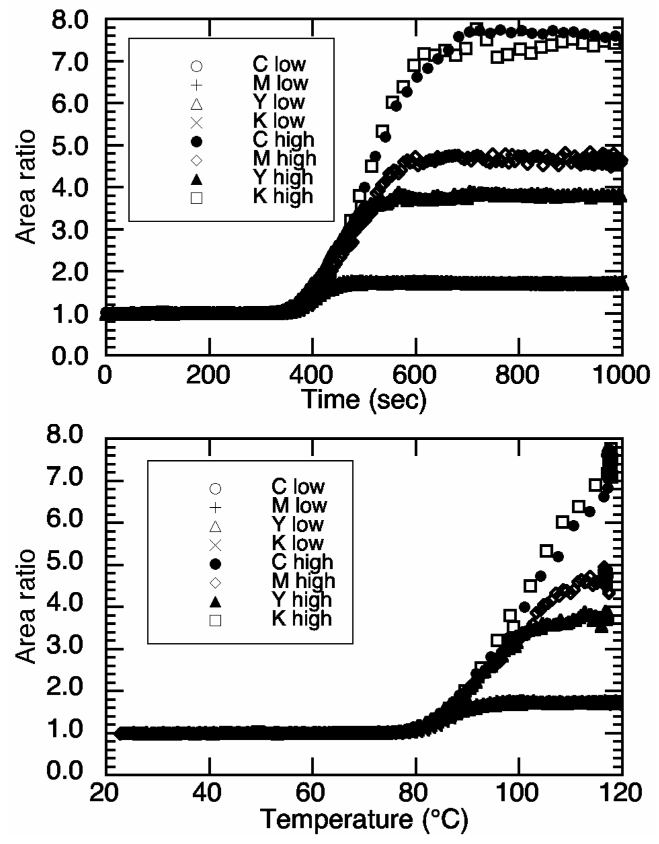

Figure 1. Area ratio of spherical toner particles of the 4 colours on hydrophobised glass (low-energy) and cleaned glass (high-energy) during the course of heating at 10°C/min, as functions of time (above), and temperature (below).

On the high-energy substrate, the spreading is far more substantial and significant differences between the 4 colours emerge. Again all colours begin spreading at this same temperature common to all 4 base polymers, and follow approximately a common slope of increase with time and temperature up to just below 100°C. However, the C and K particles then continue to spread to reach an area ratio of approx. 7.5 at 120°C. The Y particles display a plateau above 100°C, similar to the behaviour on the low-energy surface, although with a much greater spreading value. The M particle behaviour is intermediate to these two extremes.

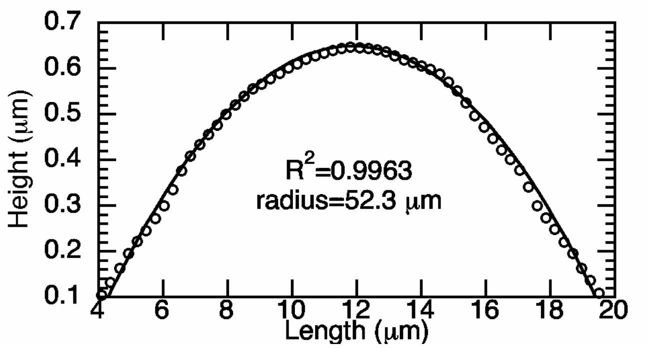

Figure 2. Height profile of a single black spherical toner particle after melting on clean glass, as measured by interferometric profilometry, showing its fit to a perfect circle arc (including coefficient of determination and circle radius).

These results clearly point to the importance and sensitivity of substrate surface chemistry. In particular, the K particles, expected from surface tension and rheology alone to exhibit least spreading, are either identical to the others or spread most, depending on the specific interactions with the substrate. To further investigate these mechanisms, the contact angles, θ_∞, of the particles in their final state are calculated from the measured area ratios (see Table 2). The calculation assumes a spherical cap geometry, which is verified by profilometric determination of the height map of toner particles in their final state, shown in Fig. 2. From the measured toner contact angles and surface tensions, γ_{lv}, the thermodynamic work of adhesion per unit area can be calculated from the Young-Dupré equation:

$$W_a = (1+\cos\theta_\infty)\gamma_{lv} \qquad (1)$$

and is also given in Table 2. The effect of the switch from hydrophobised to clean glass is a significant lowering of the contact angle and rise in the work of adhesion, together with a far greater dependence on toner type. The surface energy penalties for the low-energy substrate in contact with air and with toner are almost equally matched, irrespective of toner type, as the toner-substrate interactions are dominated by the non-polar component, approximately equal for the 4 colours. The energy cost of the toner interface with the high-energy substrate varies greatly between the toner colours. The K toner is most compatible with the cleaned glass, giving the lowest toner-substrate cost and thus more than compensating for the high cost of its interface to air. This is reflected in its highest value of work of adhesion. At the opposite extreme, the Y toner has much lower compatibility with the clean glass, so despite the benefit of low toner-air energy cost, the spreading is least. This sensitivity to toner type is due to the predominance of polar interactions between the clean glass and toner, and in particular the relatively strongly varying base component of the toner surface energy, giving high (for K) and low (for Y) affinity to the acidic glass surface.

The measured single particle spreading rates in Fig. 1 were compared to predictions from theories[1,9] using the measured equilibrium contact angle, surface tension and viscosity for the toners as input parameters. In particular, van Oene's equation for rate of area ratio (A/A_0) increase as a function of dynamic contact angle, θ, fails to correctly rank the spreading rates of the 4 toners. Instead we proposed a general empirical relation that both fits the measured data for all toner-substrate combinations and only depends on input of equilibrium contact angle and surface tension (see Fig. 3).

Table 2. Properties of the Final Spread State of the 4 Toners on the Two Substrates.

	Area ratio	Contact angle (°)	Stdv contact angle (°)	W_a (mJ/m^2)
	Hydrophobised glass			
C	1.74	84.8	2.0	38
M	1.72	85.2	2.1	36
Y	1.71	85.8	1.7	34
K	1.71	85.8	1.0	40
	Cleaned glass			
C	7.59	14.5	0.5	69
M	4.69	28.9	3.0	63
Y	3.92	36.7	1.7	57
K	7.46	14.8	1.2	74

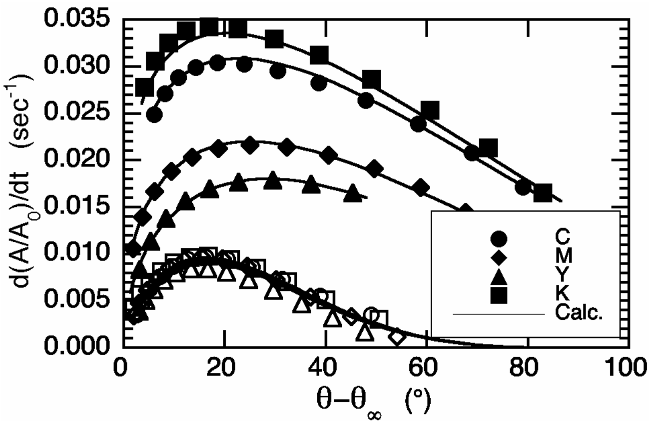

Figure 3. Spreading rates versus contact angle difference, showing experimental mean value points and calculated fitting curves, for both high-energy glass (filled symbols) and low-energy glass (unfilled symbols).

Levelling of Toner Layers

From the Xeikon printing trials, the layer thickness of the unfused full-tone areas of the 8 colour combinations is plotted in Fig. 4. The values for the single-colour layers are around 15 μm, and twice, three times and four times this thickness for the 200, 300 and 400% layers. The increasing thickness from 100% Y to C to M to K directly reflects the corresponding increase in degree of surface coverage of these particles. All thicknesses decrease on fusing, with the thicker layers exhibiting a stronger decrease. As an example, on radiant fusing of 100% and 400% black on coated paper, the thicknesses decrease exponentially with temperature from their unfused values at 70°C (polymer softening temperature) to 8 and 22 μm, respectively, at 145°C.

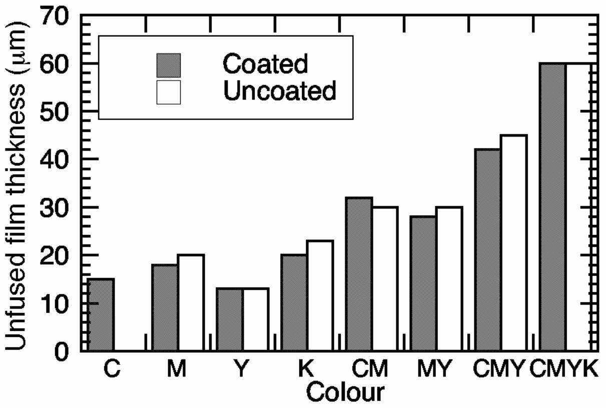

Figure 4. Mean layer thickness of unfused toner of the 8 different colour combinations on coated and uncoated paper.

Figure 5 displays the corresponding effect of the radiant fusing temperature, again without any heated nip fusing, on the high-pass filtered r.m.s. surface roughness of the printed layers on coated paper. The 100% C, M and K give similar roughness, with only a slight decrease with increasing IR temperature. The Y gives the surprising result of increasing roughness. The 200% colours give higher roughness at the low temperatures, but decrease steeply to a roughness level intermediate to the 100% and 300-400% levels. The 300% black is smoother than its 400% counterpart, and so the radiant fusing alone is insufficient to further reduce surface roughness at the highest toner amount.

Further explanation of these trends in overall roughness requires subdivision of topography into wavelength bands to pinpoint the spatial origin of the effects. For the same example of only radiant fusing of the toner layers on coated paper, Figure 6 shows two such bands. For wavelengths below 20 μm, roughness decreases with temperature due to smoothening of individual toner particle profiles and their merging with neighbours to eradicate the gaps in-between. However, Y displays the opposite trend in the 10-20 μm band, owing to its low surface coverage, hindering merging. At the higher band, 20-40 μm, the roughness of C, M and K first increases with temperature, then decreases, reflecting the continued particle and cluster merging that creates features at this length scale and which then merge further at the higher temperatures and begin contributing to the even higher band. At this highest band of 40-200 µm all colours increase their roughness with temperature due to contributions from merging at the smaller length scales, which more than outweigh the general tendency to flattening (with no nip pressure applied). For toner radiant fusing on the uncoated paper the roughness values are typically lower, owing to the melted particles' ability to partially sink into inter-fibre voids. Accordingly, the roughness increase with temperature occurs only in the highest band (40-200 µm).

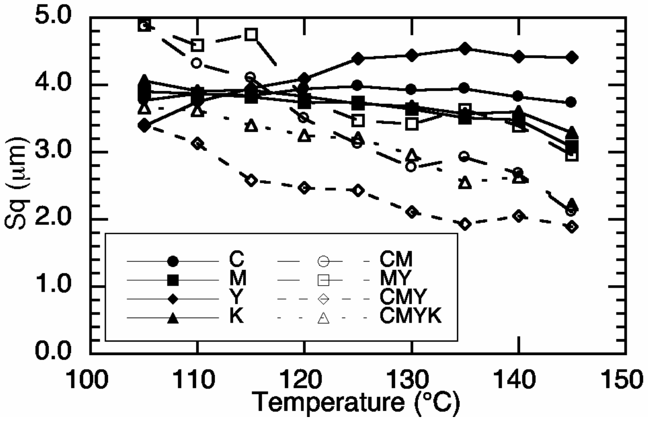

Figure 5. Total surface roughness, for wavelengths > 5 µm, of solid print areas of the 8 colour combinations on coated paper versus radiant fusing temperature, without heated roll fusing.

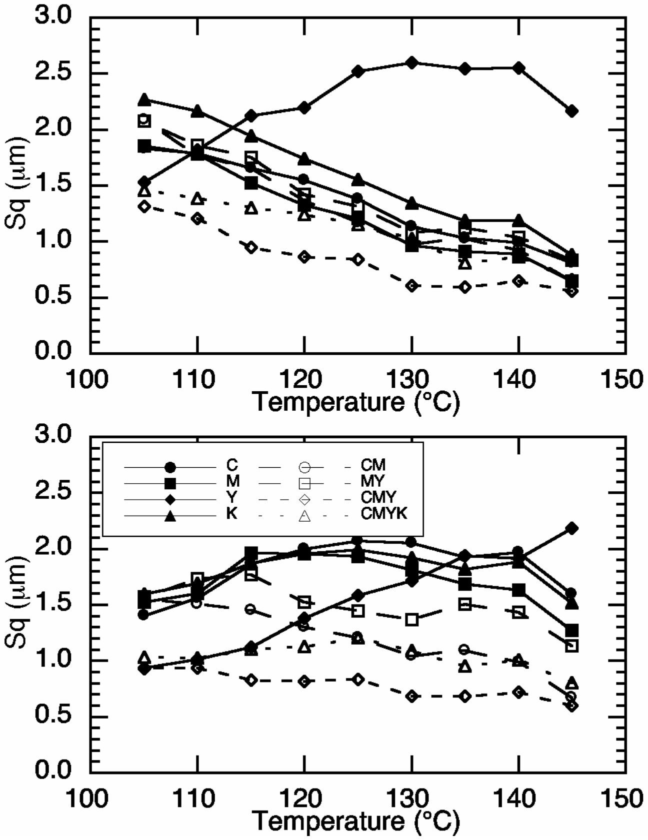

Figure 6. Surface roughness of toner films of the 8 colour combinations on coated paper, versus radiant fusing temperature (without heat rolls), showing contributions from wavelength bands 10-20 µm (above) and 20-40 µm (below).

The standard formula for gloss predicts that its logarithm decreases linearly with the square of the short-scale r.m.s. surface roughness. This theory is tested by comparing measurements of print gloss with the surface roughness bands, examples of which are shown in Fig. 7.

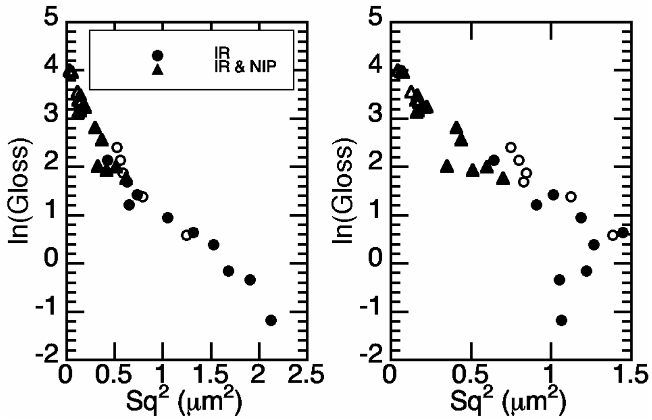

Figure 7. Log-square plot of print gloss of 400% black toner films versus surface roughness separated into wavelength bands 10-20µm (left) and 20-40µm (right). Each graph includes results on coated (filled symbols) and uncoated (open) papers, and radiant fusing alone (IR) and followed by heated roll (IR & NIP).

For all colours (excepting Y) and substrate-fusing types this log-square relation between gloss and *Sq* is approximately linear with negative slope, as expected, provided the roughness from wavelengths below 20 µm is used. This is especially clear for the print types fused only radiantly, over which a wide range of roughness and gloss values are obtained at the different temperatures. In this case the magnitude of the slope is generally greater for the uncoated paper prints, meaning that the same reduction in surface roughness (squared) gives a greater reward in gloss. This implies that some of the surface roughness due to toner particles in uncoated paper inter-fibre crevices is detected by the profilometer but not in the 75° gloss measurement. For curing with IR followed by heated roll the trends are slightly less clear, owing to the narrow range of low roughness and high gloss obtained, due to the high radiant temperatures used plus the added effect of the rolls. However it appears that the slopes in these cases are also high, at roughly the level of those for purely IR fusing on uncoated paper. The extra glossing benefit of the heated rolls is the direct result of toner particle flattening, on the micro-scale, as well as increasing orientation over more macro-scales to increase the number of areas contributing to the same 75° reflection.

For the wavelength band 20-40 μm, the correlation between gloss and surface roughness persists for all colours (excepting Y) and for all substrate-fusing types excluding purely IR fusing on coated paper. The latter gives poor correlation for the colours in Fig. 6 for which this band does not give decreasing roughness with increasing IR temperature. In particular, the low fusing temperatures give low roughness values since the particles have not merged sufficiently to give sizes contributing to this band, however the gloss is still very low, as apparent from the particles' contribution to lower wavelength roughness. The low physical coverage of Y results in weaker gloss-roughness correlations and different results for the different fusing types, since melting-induced merging is limited and only the nip pressure is capable of flattening the isolated particles.

Figure 8 summarises the correlation between the printed paper gloss and surface roughness in all 5 bands. The maximum length scales over which the correlation persists clearly increase with degree of toner coverage or layer thickness, i.e. from Y to C to M and K to the 200-400% print layers. This correlation length also tends to increase from coated to uncoated paper, and from radiant fusing alone to its combination with the heated rolls.

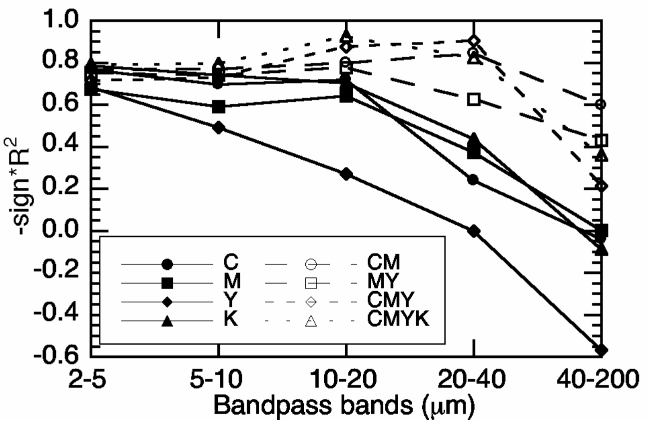

Figure 8. Coefficient of determination, R^2, of the least-squares fits of the gloss-roughness log-square plots to straight lines, for all 8 colour combinations, averaged over both coated paper and uncoated paper and both fusing combinations. The coefficient varies from +1, indicating fit to a negatively sloping line, to –1, indicating fit to a positively sloping line.

Conclusion

This study has developed a relatively simple instrument to in-situ image and quantify the spreading of individual toner particles. Although the method was mainly applied to spherically-transformed particles, the spreading of irregular ground particles has also been successfully quantified. Similarly, the use of smooth and inert model substrates of well-defined surface chemistry paves the way for interpreting behaviour on real electrophotographic media. As expected, the high-energy substrate exhibited far greater spreading, and work of adhesion generated by it, and also a much stronger dependence on the toner type. For these Xeikon toners the C and K spread far more than the M, with Y clearly the lowest. One possible extension is to employ a set of model substrates representing individual components of the complex real substrate, to separately examine each component's influence on spreading and related properties.

This study has also illustrated the utility of the white-light interferometric profilometer in quantifying the thickness and surface roughness spectral decomposition of toner layers transferred and fused on paper substrates, thus giving increased insight into the mechanisms giving rise to toner print quality. Although the transferred toner amount is clearly the most important input material parameter, it is possible that the varying chemistries and particle spreading abilities of the 4 toners also contributes to the observed differences. It would thus be of interest to study, with this profilometric technique, the fusing behaviour of these 4 colours, not at their standard optical densities (as performed here), but rather at constant equal physical coverage.

References

1. Lee, L.H., Thermal fixing of electrophotographic images, in Adhesion science and technology, L.H. Lee, Editor. 1975, Plenium Press, New York, pg. 831 - 852.
2. Sipi, K.M., et al., Journal of Imaging Science and Technology, 44(5), 442 (2000).
3. Sipi, K.M., et al., Print quality in contact and non-contact fixing, IS&T's NIP 15, pg. 426 (1999).
4. Prime, R.B., Photographic science and engineering, 27(1), 19 (1983).
5. Briggs, J.C., et al., The effect of fusing on gloss in electrophotography, IS&T's NIP 14, pg. 456 (1998).
6. Drelich, J., et al., Journal of Colloid and Interface Science, 201(2), 253 (1998).
7. Eriksson, J., et al., Langmuir, 17(23), 7274 (2001).
8. Segeren, L., et al., Journal of Chromatography A, 969(1-2), 215 (2002).
9. Van Oene, H., et al., Journal of Adhesion, 1, 54 (1969).

Biography

Torbjorn Pettersson is employed as a PhD student within the Forest Products Section at the Institute for Surface Chemistry (YKI), in Stockholm, Sweden. He has worked for the past 4 years with surface chemical aspects of electrophotographic printing techniques, including optical properties, adhesion and friction. He received his M.Sc. in chemistry from Stockholm University in 2000, and is planning to complete his PhD thesis during 2005.